Molecular Crystals and Liquid Crystals

Publication details, including instructions for authors and subscription information:
http://www.tandfonline.com/loi/gmcl20

Defects Nucleation and Dynamical Behavior from Surface Inhomogeneity

Gi-Dong Lee [a], Jong Wook Lee [b], Kyoung-Ho Park [b], Jae Chang Kim [b], Tae Woon Ko [c], Joun Ho Lee [c], Chang Ho Oh [c] & Hyun Chul Choi [c]

[a] Divison of Electronics Engineering, Dong-A University, Busan, Korea

[b] Department of Electronics Engineering, Pusan National University, Busan, Korea

[c] LG. Philips LCD, Jinpyung-dong, Gumi-city, Kyungbuk, Korea

Version of record first published: 31 Aug 2006.

To cite this article: Gi-Dong Lee, Jong Wook Lee, Kyoung-Ho Park, Jae Chang Kim, Tae Woon Ko, Joun Ho Lee, Chang Ho Oh & Hyun Chul Choi (2005): Defects Nucleation and Dynamical Behavior from Surface Inhomogeneity, Molecular Crystals and Liquid Crystals, 433:1, 199-206

To link to this article: http://dx.doi.org/10.1080/15421400590956676

Mol. Cryst. Liq. Cryst., Vol. 433, pp. 199–206, 2005

ISSN: 1542-1406 print/1563-5287 online
DOI: 10.1080/15421400590956676

Taylor & Francis
Taylor & Francis Group

Defects Nucleation and Dynamical Behavior from Surface Inhomogeneity

Gi-Dong Lee
Divison of Electronics Engineering, Dong-A University, Busan, Korea

Jong Wook Lee
Kyoung-Ho Park
Jae Chang Kim
Department of Electronics Engineering, Pusan National University, Busan, Korea

Tae Woon Ko
Joun Ho Lee
Chang Ho Oh
Hyun Chul Choi
LG. Philips LCD, Jinpyung-dong, Gumi-city, Kyungbuk, Korea

We model the nucleation and dynamical behavior of defects from an inhomogeneous surface configuration using fast Q-tensor method. A fast Q-tensor method, which can model the defect dynamics in a liquid crystal director field, is applied to model the defect nucleation and dynamics. From the numerical modeling, we confirmed that surface inhomogeneity which makes strong strain energy in the local liquid crystal director field could cause defects. Experimental result has compared with numerical modeling in order to verify the simulation of the defect nucleation.

Keywords: defect; liquid crystal; surface inhomogeneity

1. INTRODUCTION

An understanding of the dynamical behavior of liquid crystal director including defects and transitions between topologically inequivalent states has become important for advanced liquid crystal modes, which

Address correspondence to Gi-Dong Lee, Department of Electronics Engineering, Dong-A University, Busan, 604-714, Korea. E-mail: gdlee@daunet.donga.ac.kr

can exhibit excellent electro-optical characteristics, such as in-plane switch cell, patterned vertically aligned cell, multi-domain cell and so on. In order to understand defect dynamics, generally, two and three dimensional calculations that can include disclination for liquid crystal cells are important.

In previous papers [1,2] we introduced fast Q-tensor method which can handle defect dynamics in addition to normal liquid crystal behavior and topological transition. Dickman had shown that Oseen–Frank vector representation could go directly to the Q-tensor representation if we use only one 3rd order Q component [3]. However, Dickman considered only a constant value of order parameter S, so that the results are only qualitative in their description of defects. We have successfully shown that the fast Q-tensor method calculate the order parameter by adding the temperature terms in addition to the Q-tensor representation of Oseen-Frank free energy terms [1]. Besides, we have derived an improved normalization method for the faster calculations.

Defects in the LC director field sometimes are occurred due to surface inhomogeneity in addition to topologically inequivalent transition, because it can derive high elastic energy around at "high changed position". Figure 1 is a cartoon that shows the defect nucleation and defect lines at prominence of the surface in the homeotropic aligned liquid crystal director field [4].

In this paper, we model the defect from surface prominence shown in Figure 1 using fast Q-tensor representation. In order to confirm the calculated result, we compared the numerical modeling of the defect nucleation with experimental phenomenon. In addition, dynamical behaviors of the defect from surface inhomogeneity have calculated under applied voltages.

2. NUMERICAL MODELING OF A FAST Q TENSOR METHOD

The Gibb's free energy density (f_g) consists of elastic energy density term of LC director (f_s) and external electric free energy density term (f_e). Simply, we can achieve the total energy by integrating the

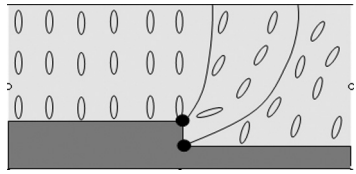

FIGURE 1 An example of the decoration of mechanical inhomogeneities at a prominence by a nematic liquid crystal.

calculated Gibb's free energy density. As I mentioned above, Dickman successfully derived the Q-tensor form from the vector form of the Frank–Oseen strain free energy density as below [5],

$$\begin{aligned} fs &= \frac{1}{12}(k_{33}-k_{11}+3k_{22})\frac{G_1^{(2)}}{S^2}+\frac{1}{2}(k_{11}-k_{22}-3k_{24})\frac{G_2^{(2)}}{S^2} \\ &\quad +\frac{1}{2}k_{24}\frac{G_3^{(2)}}{S^2}+\frac{1}{6}(k_{33}-k_{11})\frac{G_6^{(3)}}{S^3}+q_0k_{22}\frac{G_4^{(2)}}{S^2} \\ G_1^{(2)} &= Q_{jk,l}Q_{jk,l}, G_2^{(2)} = Q_{jk,k}Q_{jl,l} \\ G_3^{(2)} &= Q_{jk,l}Q_{jl,k}, G_4^{(2)} = e_{jkl}Q_{jm}Q_{jm,l} \\ G_6^{(3)} &= Q_{jk}Q_{lm,j}Q_{lm,k} \end{aligned} \tag{1}$$

where $Q_{jk} = S(n_jn_k - \frac{\delta_{jk}}{3}), Q_{jk,l} = \frac{\partial Q_{jk}}{\partial l}$

The electric free energy density for the Q-tensor form is derived directly from $f_e = D{\cdot}E/2$. From this, the Q-tensor form for the electric free energy density can be obtained as below [5],

$$f_e = \frac{1}{2}\varepsilon_0\left(\bar{\varepsilon}V_j^2 + \Delta\varepsilon V_{,j}V_{,k}\frac{Q_{jk}}{S}\right) = \frac{2\varepsilon_\perp+\varepsilon_c}{3}, \Delta\varepsilon = \varepsilon_\perp - \varepsilon_c, V_{,j} = \frac{\partial V}{\partial j} \tag{2}$$

In order to calculate order parameter S in each grid, we need to add a temperature energy term that, in the absence of director field distortion, determine S as a function of temperature because the order parameter S is related directly to temperature. Basically, we can formulate the thermal energy density by using a simple polynomial expansion which is expressed as follows [6],

$$\begin{aligned} f_t(T) &= fo + \frac{1}{2}A(T)Q_{ij}Q_{ji} + \frac{1}{3}B(T)Q_{ij}Q_{jk}Q_{ki} \\ &\quad + \frac{1}{4}C(T)(Q_{ij}Q_{ij})^2 + O(Q^5) \end{aligned} \tag{3}$$

Therefore, the total free energy density is the sum of equations (1), (2) and (3), so that the Gibb's free energy density can be described as the sum of these three energy densities.

In order to achieve the equilibrium state of the director configuration at constant electric field, it is typical to use the Euler–Lagrange equation. The following equations show the Euler–Lagrange representation for the electric potential and the director components under the Cartesian coordinate system. By solving Eq. (4), potential distribution

and LC configurations can be obtained, respectively.

$$0 = -[f_g]_{Q_{jk}}$$
$$0 = -[f_g]_V = \nabla \cdot D$$

where

$$[f_g]_{Q_{jk}} = \frac{\partial f_g}{\partial Q_{jk}} - \frac{d}{dx}\left(\frac{\partial f_g}{\partial Q_{jk,x}}\right) - \frac{d}{dx}\left(\frac{\partial f_g}{\partial Q_{jk,y}}\right) - \frac{d}{dx}\left(\frac{\partial f_g}{\partial Q_{jk,z}}\right)$$
$$[f_g]_V = \frac{\partial f_g}{\partial V} - \frac{d}{dx}\left(\frac{\partial f_g}{\partial V_{,x}}\right) - \frac{d}{dx}\left(\frac{\partial f_g}{\partial V_{,y}}\right) - \frac{d}{dx}\left(\frac{\partial f_g}{\partial V_{,z}}\right) \quad (4)$$

The terms $[f_g]_{Qjk}$ and $[f_g]_V$ represent the functional derivatives with respect to the Q_{jk} and voltage V, respectively. By using these equations, we can calculate the components of the 3 by 3 Q matrix and voltages in each grid. Functional derivatives by each energy term are described as follows [2],

$$[f_g]_{Qjk} = \text{strain term}([f_g]_S) + \text{voltage term}([f_g]_V) + \text{temperature term}([f_g]_T)$$

$$\begin{aligned}[f_g]_S = &-\frac{2}{S^2}\left(-\frac{1}{12}K_{11} + \frac{1}{4}K_{22} + \frac{1}{12}K_{33}\right)Q_{jk,ll} + \frac{(K_{11}-K_{22})}{S^2}Q_{jl,lk} \\ &- \frac{K_{24}}{S^2}Q_{jl,lk} + \frac{1}{4S^3}(K_{33}-K_{11})(Q_{lm,j}Q_{lm,k} - Q_{lm,l}Q_{jk,m} \\ &- Q_{lm}Q_{jk,ml} - Q_{lm,m}Q_{jk,l} - Q_{lm}Q_{jk,lm}) \\ &+ \frac{2}{S^2}q_0 K_{22} e_{jlm} Q_{mk,l} \qquad (5)\end{aligned}$$

$$[f_g]_V = -\frac{1}{2}e_0 D_e V_{,j} V_{,k}$$

$$[f_g]_T = (A_1 + A_2\frac{T}{T_{ni}})Q \cdot Q + A_3 Q \cdot Q \cdot Q + A_4 Q \cdot Q \cdot Q \cdot Q$$

$$Q_{jk,ll} = \frac{\partial}{\partial l}\left(\frac{\partial Q_{jk}}{\partial l}\right)$$

where, T is current temperature, T_{n_i} represents the nematic-isotropic transition temperature, and the constants from A_1 to A_4 represent the coefficients for the polynomial equation. Generally, polynomial coefficients may be dependent on nematic material. The polynomial coefficients A_1 to A_4 have been adjusted so the T_{ni} as to be around 95°C, so that we can see order parameter S and all diagonalzed Q components

go to 0 at T_{ni} from typical value of room temperature (25°C). As a result, we calculated that tha polynomial coefficients A_1, A_2, A_3 and A_4 are $0.79\,\mathrm{J/cm^3}$, $0.784\,\mathrm{J/cm^3}$, $0.61\,\mathrm{J/cm^3}$ and $1.474\,\mathrm{J/cm^3}$, respectively.

The dynamic equation $\gamma\,(\partial Q_{jk}/\partial t) = -[f_g]_{Qjk}$ can provide the equilibrium state by recalculating the Q-tensor and voltages in every time step in each grid. γ is rotational viscosity and we ignored bulk viscosity because have not considered flow effect. To obtain an equilibrium state, we applied relaxation method based on dynamic equation for numerical calculation. As a result, the formulated relation between Q tensor of next time $Q_{jk}^{-\tau+1}$ and that of current time $Q_{jk}^{-\tau}$ is as follows,

$$Q_{jk}^{-\tau+1} = Q_{jk}^{-\tau} + \frac{\Delta t}{\gamma}[f_g]_{Q_{jk}} \tag{6}$$

The order parameter S is related to Q-tensor in the equation by $S^2 = 1.5(\mathbf{Q}\cdot\mathbf{Q})$ and we can get this simultaneously with the Q components.

3. NUMERICAL MODELING FOR THE DEFECT NUCLEATION AND DYNAMICAL BEHAVIORS

De Gennes mentioned that the size of the defect core might be approached to molecular dimensions [6], so that we may encounter a serious problem for observing the defect core in the LC configuration. In the previous papers [1,2] we proposed a numerical method to find defect core out by reducing the temperature coefficients $A1$ to $A4$. Otherwise, we need to scale down the cell structure for calculation. These two approaches obviously allow us to observe defect generation and dynamics.

Figure 2(a) shows the geometry of the vertical aligned cell to realize the cell structure as shown in Figure 1. Used liquid crystal material was MLC-6608 of Merck company ($K_{11} = 16.7\,\mathrm{pN}$, $K_{22} = 7.3\,\mathrm{pN}$, $K_{33} = 18.1\,\mathrm{pN}$, $\varepsilon_{\square} = 3.6$, $\varepsilon_{\perp} = 7.8$). Cell gap to keep LC layer was 5 μm, and ZnO layer was used for step surface configuration in a z-direction. Height of the ZnO layer was 1 μm. Figure 2(b) shows microscopic photograph of the cell with crossed polarizers. From the figure, we have observed the light leakage from the edge of the electrode which implies nucleation of the defect core due to surface inhomogeneity with step type of the edge.

Figure 3 shows the cell geometry for simulating the defect nucleation from surface inhomogeneity. For the calculation, the number of calculated layers was set to 50×50 in the x and z directions. LC directors on both surfaces have aligned vertically and we assumed

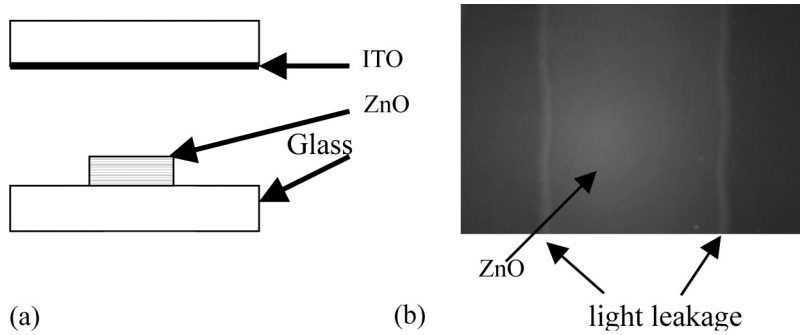

FIGURE 2 An experiment for observing defect nucleation; (a) cell structure, (b) light leakage under crossed polarizers.

that the LC directors at corner grids of the edge have average numerical values of the neighbor directors as shown in Figure 3 (b).

Figure 4 shows calculated result using fast Q-tensor method. In the figure, length of the lines is proportional to amplitude of S, so that circled areas in the figure imply the points of defect nucleation. Without applied voltage as shown in Figure (a), defect was nucleated along z-axis at step side. This implies that high strain energy may be stored along z-axis at step side because the LC directors along surface in the z-axis meet LC directors in bulk area with perpendicular state in a very short range. Figure 4 (b), (c) and (d) show the dynamical behavior of the generated defects from surface inhomogeneity. The defect line in the Figure 4 (b) is generated from the edge of the electrode because of high strain energy, which was predicted in Figure 1. It moves to the bulk area along defect line by applying the electric field.

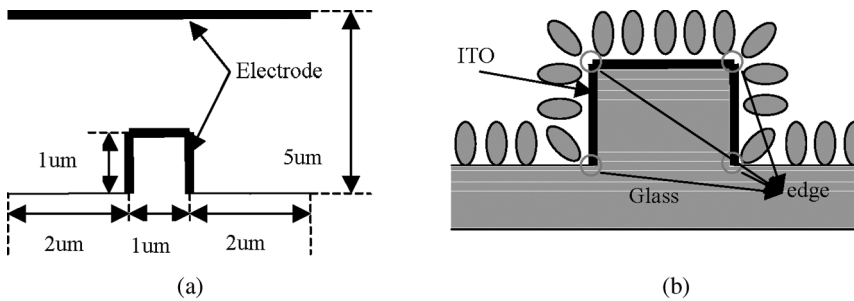

FIGURE 3 The geometry of a vertical alignment LC cell for calculation; (a) cell structure, (b) LC alignment on the inhomogeneous surface.

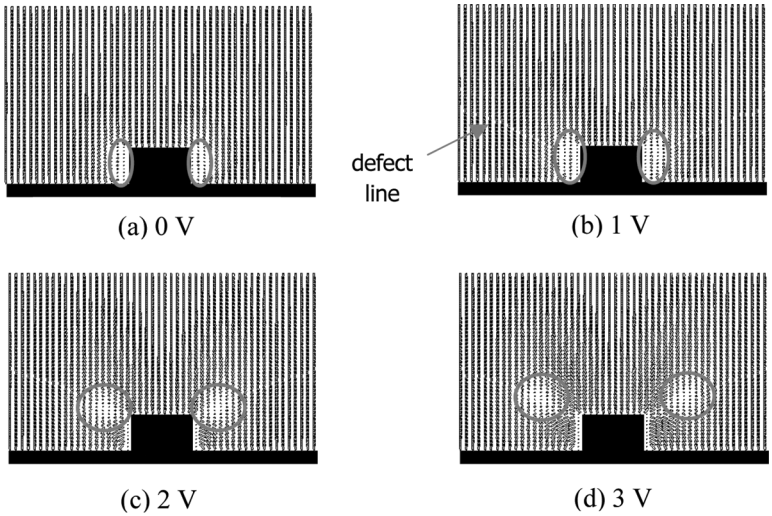

FIGURE 4 Two-dimensional director configurations under applied voltage for a vertical alignment cell; (a) 0 V, (b) 1 V, (c) 2 V, (d) 3 V. The orientations of the cylinders give the local director orientation, which has very small scalar order parameter S.

However, moving distance of the defects may be very short (under several μm), so that we assume that the generated defects due to step surface inhomogeneity look stuck around the edge of the electrode even if we apply electric field.

4. CONCLUSIONS

Numerical modeling of the liquid crystal defect from surface inhomogeneity has been presented by using fast Q-tensor method. We confirmed the defect has been nucleated around edge of the electrode and it moved along the defect line into LC bulk area. For better optical characteristics of the LC cell, various structure of the LC cell may be applied to LC optical design and this may cause the unpredictable optical loss because of generated defects. A Fast Q-tensor method which provides information of order parameter S may help us to understand defect dynamics and to design LC cell better.

REFERENCES

[1] Lee, G.-D., Anderson, J., & Bos, P. J. (2002). *Applied Physics Lett.*, *81*, 3951.
[2] Lee, G. D., Bos, P. J., Ahn, S. H., & Kim, K. H. (2003). *Phys. Rev. E*, *67*, 041715.

[3] Dickmann, S. (1995). Ph.D. Dissertation, University Karlsruhe, Karlsruhe, Germany.
[4] Sonin, A. A. (1995). *The Surface Physics of Liquid Crystals*, Gordon and Breach Publishers.
[5] Mori, H., Gartland, E. C., Kelly, J. R., & Bos, P. J. (1999). *Jpn. J. Appl. Phys.*, *38*, 1999.
[6] de Gennes, P. G. & Prost, J. (1993). *The Physics of Liquid Crystals*, Clarendon Press, Oxford 2ed.